25th ABCM International Congress of Mechanical Engineering
October 20-25, 2019, Uberlândia, MG, Brazil

COB-2019-0734
IDENTIFICATION OF THE MUSAT SPHERICAL SATELLITE ATTITUDE SIMULATOR MASS PROPERTIES USING THE EXTENDED KALMAN FILTER

Rômulo Fernandes da Costa
Osamu Saotome
Instituto Tecnológico de Aeronáutica, 50, Vila das Acacias, São José dos Campos – SP, Brazil
elromulo2006@yahoo.com.br / osaotome@ele.ita.br

Alain Giacobini de Souza
Instituto Tecnológico de Aeronáutica, 50, Vila das Acacias, São José dos Campos – SP, Brazil
alaingiacobini@gmail.com

Luiz Carlos Sandoval Góes
Instituto Tecnológico de Aeronáutica, 50, Vila das Acacias, São José dos Campos – SP, Brazil
goes@ita.br

Ijar Milagre da Fonseca
Instituto Tecnológico de Aeronáutica, 50, Vila das Acacias, São José dos Campos – SP, Brazil
ijar.fonseca@gmail.com

Abstract. *This paper presents the identification of the inertia matrix and the center of mass from the satellite attitude dynamics simulator (SADS) platform developed by ITA, named MuSat, using the extended Kalman filter. This platform consists on a sphere suspended by an air bearing, which allows the sphere to rotate frictionless in all three axes. The sphere contains three orthogonally oriented reaction wheels for exerting torque on the system, and a 9-degrees of freedom inertial measurement unit (9-DOF IMU), which will be used for acquiring attitude data from the sphere. The reaction wheels are used for exciting all modes of the system, and the attitude response measured by the IMU is used for estimating the system parameters.*

Keywords: *System Identification, Extended Kalman Filter, Satellite Attitude Dynamics Simulator.*

1. INTRODUCTION

The problem of satellite dynamics and control is one of the main topics of research work at ITA, given its mission of training personnel for working in the aerospace industry. One of the most critical parts for the correct functioning of a satellite is the attitude control system (ACS), which is responsible for the adjustment of orientation of the satellite in space. A precise ACS is required for the correct pointing of antennas, of solar panels for recharging batteries, and for trajectory adjustment.

For the purposes of validating satellite ACS and demonstrating satellite dynamics for students, a spherical satellite attitude dynamics simulator (SADS) platform has been developed by the institution, as documented in (Figueiredo and Saotome, 2013) and (Silva et al., 2014). This SADS platform was named MuSat (short for "Mock-Up Satellite"), and it consists on a sphere suspended in a very thin layer of air by a spherical air bearing, so that the sphere is free to rotate in three axes. It also has a set of three reaction wheels as actuators and an inertial measurement unit (IMU) for attitude acquisition. Its functioning has been demonstrated in the works of (Silva et al., 2014), (Costa and Saotome, 2016), and (Costa and Saotome, 2018).

Due to the precise nature of satellite attitude control problem, it is necessary to have an accurate measurement of the satellite's mass properties, such as the center of mass and inertia matrix. The mass properties of the MuSat were initially estimated by CAD software during the manufacturing process. These initial estimates were used on the MuSat's computational model for numerical simulation (Silva et al., 2014) and for designing new control schemes for the MuSat's sphere (Costa and Saotome, 2018).

However, due to eventual modifications made on the MuSat physical simulator (the sphere) over the years, such as the replacement of internal batteries, modifications on the wiring and communication devices, the mass properties of the

system have changed from those initially estimated during the project. This may lead to dissonance between the computational model used for numerical simulation and results obtained from the physical simulator.

This work demonstrates the usage of the actuators and tools already present on the platform for identification of the system parameters. The reaction wheels are used for exciting the system, and the attitude response is then measured by the sensors in the sphere. The Extended Kalman Filter (EKF) will be used to determine the correct parameters of the system, as it can be used as an estimator of the states and the parameters of a nonlinear system.

2. THE MUSAT SATELLITE ATTITUDE DYNAMICS SIMULATOR

2.1 Description of the MuSat Test Bed

The MuSat test bed is a SADS platform, designed by the Laboratory of Space Robotics at ITA, for performing satellite attitude control experiments on laboratory, such as testing, validating and comparing the performance of non-linear control schemes, and demonstrating the effects of gyroscopic and gravitational torques present on satellite attitude dynamics. The MuSat consists on an air bearing that maintains an aluminum sphere floating over a very thin layer of air. This creates a nearly frictionless environment in which the sphere is free to rotate in three axes, limited only by the edges of the bearing.

Internally there are three orthogonally orientated reaction wheels aligned with each axis of rotation of the sphere, functioning as actuators for attitude control. Each reaction wheel comprises a 3242G012BX4 brushless motor and its motion controller device, sold by Faulharber. The motion controller devices are responsible for driving the motors of each wheel to a given velocity and providing measurement of their current velocity. By commanding the motors' motion controller to accelerate or decelerate a wheel, torque can be imposed on the sphere, which will cause the sphere to rotate over the bearing.

Atop the sphere, there's a lid containing a single GY-80 Inertial Measurement Unit (IMU). This IMU contains a three-axis magnetometer, a three-axis accelerometer and a three-axis gyro sensor, which are used in the experiment for acquiring the sphere's current attitude and angular velocity. The lid also contains two counterweights, which can be used to manually adjust the position of the center of gravity of the sphere.

An Arduino Mega Board manages the data acquired by the IMU and each one of the reaction wheel's controllers. Communication with the IMU is done over the I^2C protocol, while the RS-232 standard is used for communicating with the reaction wheels' motion controllers. Additionally, the Arduino Mega is also responsible for establishing wireless communication through WiFi with an external computer. An ESP-8266 is used as a WiFi Module for the Arduino.

The computer will act as a ground station for the SADS. The program executed on the computer logs and displays the data transmitted by the MuSat sphere, which contains the current attitude, angular velocity and the wheels velocities. It can also execute an attitude control algorithm defined by the user, so that the reaction wheels are accelerated or decelerated accordingly to the control laws defined in the program. The calculated acceleration for all three wheels are numerically integrated within the program, and are then transmitted back to the MuSat as velocity commands, therefore closing a control loop.

Figure 1 shows a photograph taken of the sphere rotating over the air bearing, along with a computer running a control algorithm designed in MATLAB. Figure 2 presents a block diagram of the MuSat system, presenting a general overview of the system including the external controller algorithm.

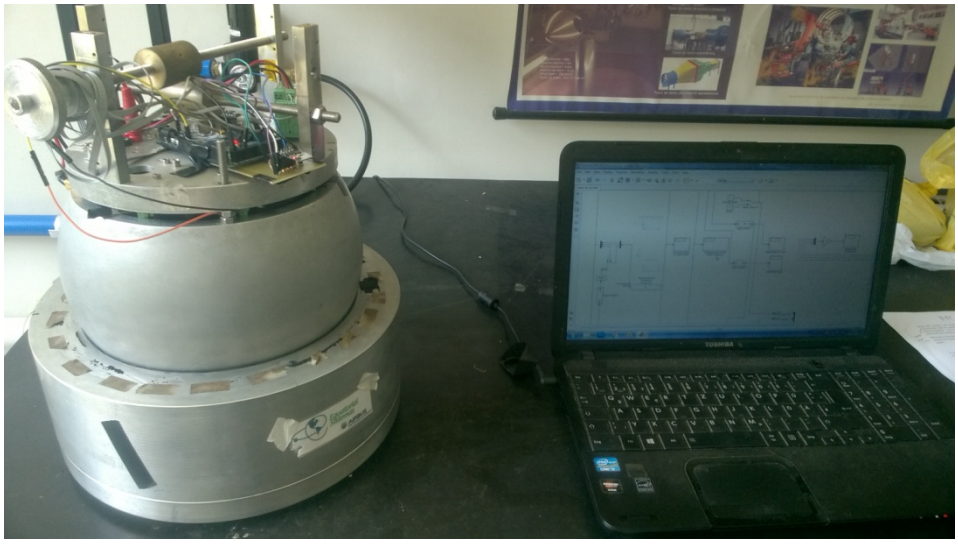

Figure 1. Photograph of MuSat Sphere over the air bearing.

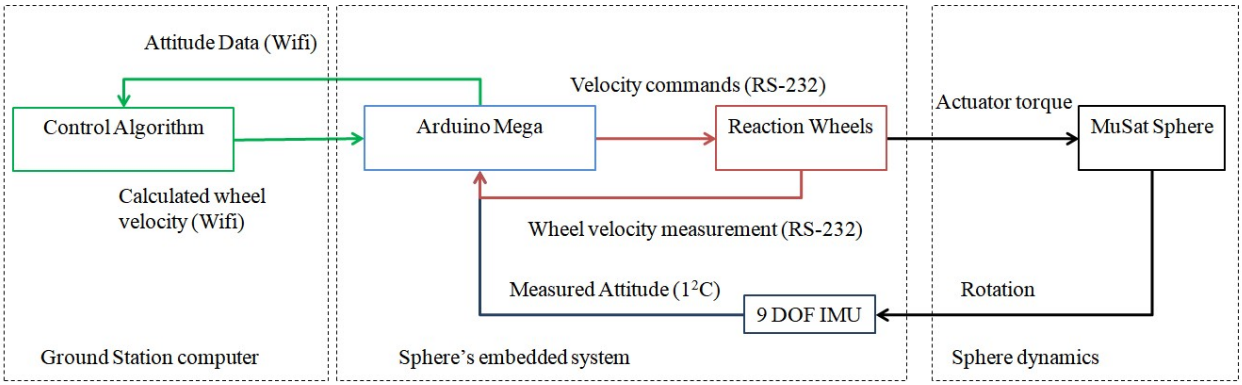

Figure 2. Block diagram of the MuSat system.

2.2 System dynamics

The coordinate system used in the following equations follows the Local NED (North-East-Down) convention commonly used in aeronautics. The origin is located at the center of rotation of the sphere, with the x-axis pointing forward, the Y-axis pointing towards the right, and Z-axis points downwards.

The dynamics of the MuSat sphere can be derived from the summation of all the torques acting on the system. Consider the system's total angular momentum vector $\boldsymbol{H}$:

$$\boldsymbol{H} = \boldsymbol{H_{sphere}} + \boldsymbol{H_{wheels}} = \boldsymbol{I_{sphere}}\boldsymbol{\omega} + \boldsymbol{J_{wheels}}(\boldsymbol{\Omega} + \boldsymbol{\omega}) = \boldsymbol{I_{system}}\boldsymbol{\omega} + \boldsymbol{J_{wheels}}\boldsymbol{\Omega} \tag{1}$$

Where $\boldsymbol{H_{sphere}}$ and $\boldsymbol{H_{wheels}}$ are the angular momentum of the sphere and the wheels respectively, $\boldsymbol{I_{system}}$ is the combined inertia matrix of the system (sphere's body and wheels), $\boldsymbol{I_{sphere}}$ and $\boldsymbol{J_{wheels}}$ are the sphere's and the wheels' moment of inertia respectively. The vectors $\boldsymbol{\omega} = [\omega_x \omega_y \omega_z]^T$ and $\boldsymbol{\Omega} = [\Omega_x \Omega_y \Omega_z]^T$ represent the angular velocity of the sphere and relative angular velocity of the reaction wheels. Both $\boldsymbol{\omega}$ and $\boldsymbol{\Omega}$ are represented in the sphere's body coordinate system.

The external torque acting on the sphere $\boldsymbol{T_{ext}}$ is obtained from Euler's angular momentum equation (Sidi, 1997), as shown in Eq. (2). By isolating $\dot{\boldsymbol{\omega}}$, one obtains the angular acceleration of the system.

$$\boldsymbol{T_{ext}} = \dot{\boldsymbol{H}} + \boldsymbol{\omega} \times \boldsymbol{H} = \boldsymbol{I_{system}}\dot{\boldsymbol{\omega}} + \boldsymbol{J_{wheels}}\dot{\boldsymbol{\Omega}} + \boldsymbol{\omega} \times \boldsymbol{I_{system}}\boldsymbol{\omega} + \boldsymbol{\omega} \times \boldsymbol{J_{wheels}}\boldsymbol{\Omega} \tag{2}$$

$$\dot{\boldsymbol{\omega}} = \boldsymbol{I_{system}}^{-1}[\boldsymbol{T_{ext}} - \boldsymbol{J_{wheels}}\dot{\boldsymbol{\Omega}} - (\boldsymbol{\omega} \times \boldsymbol{I_{system}}\boldsymbol{\omega}) - (\boldsymbol{\omega} \times \boldsymbol{J_{wheels}}\boldsymbol{\Omega})] \tag{3}$$

In this paper, it is assumed that the external torque $\boldsymbol{T_{ext}}$ is caused solely by gravitational torque, that is, the misalignment of the center of mass with respect to the center of rotation of the sphere. Therefore $\boldsymbol{T_{ext}}$ can be calculated by:

$$\boldsymbol{T_{ext}} = \boldsymbol{r_{CM}} \times m\boldsymbol{g} = m.|g| \begin{bmatrix} r_y \cos\phi \cos\theta - r_z \sin\phi \cos\theta \\ -r_z \sin\theta - r_x \cos\phi \cos\theta \\ r_x \sin\phi \cos\theta + r_y \sin\theta \end{bmatrix} \tag{4}$$

where $\boldsymbol{r_{CM}} = [r_x, r_y, r_z]^T$ .is the position of the center of mass of the sphere, m is the MuSat's combined mass, and $\boldsymbol{g}$ is the gravity vector represented in the sphere's body coordinate system. Decomposing the cross product in Eq. (4) yields the vector seen on right side of the equation.

In order to convert the angular rate vector $\boldsymbol{\omega}$ to Euler angular rates $[\dot{\phi}\ \dot{\theta}\ \dot{\psi}]^T$ (in which the vector $[\phi\ \theta\ \psi]^T$ contains the Euler angles roll, pitch and yaw respectively), the conversion matrix shown in Eq. (5) must be applied.

$$\begin{bmatrix} \dot{\phi} \\ \dot{\theta} \\ \dot{\psi} \end{bmatrix} = \begin{bmatrix} 1 & sin\phi tan\theta & cos\phi tan\theta \\ 0 & cos\phi & -sin\phi \\ 0 & \frac{sin\phi}{co} & \frac{cos\phi}{co} \end{bmatrix} \begin{bmatrix} \omega_x \\ \omega_y \\ \omega_z \end{bmatrix} \tag{5}$$

3. EXTENDED KALMAN FILTER

3.1 Definition

The extended Kalman filter (EKF) is a well known algorithm used primarily for estimating the current state variables of a nonlinear system. Like the traditional Kalman filter, it provides an accurate estimation of the states of a given system in two iterative steps: the time propagation or prediction step, in which the current state is estimated by using a linearized model of the system, and the measurement update step, in which the prediction is corrected by considering the uncertainty of the linearized model and the uncertainty present on the measurement. The EFK can be modified for estimating parameters of the system as well, by treating the system parameters to be identified as part of the state vector estimated by the EKF.

Consider the following representation of nonlinear system $\boldsymbol{x_k}$ at the instant $\boldsymbol{t_k}$, with parameters represented by $\boldsymbol{\Theta_k}$ and known inputs $\mathbf{u_k}$,given by

$$\dot{\boldsymbol{x_k}} = \boldsymbol{f}(\boldsymbol{x_k}, \boldsymbol{u_k}, \boldsymbol{\Theta}_\mathbf{k}) + \boldsymbol{w_x} \tag{6}$$

where $\boldsymbol{f}(\boldsymbol{x_k}, \boldsymbol{u_k}, \boldsymbol{\Theta}_\mathbf{k})$ is a nonlinear function and $\boldsymbol{w_x}$ is an set of unknown inputs.

Likewise, assume that there's a set of measurements, $\boldsymbol{y_k}$, obtained by sensors modeled by $\boldsymbol{h_k}$ and corrupted by sensor noise signal $\boldsymbol{v_k}$:

$$\boldsymbol{y_k} = \boldsymbol{h_k}(\boldsymbol{x_k}) + \boldsymbol{v_k} \tag{7}$$

The Extended Kalman Filter can then be summarized by a set of five equations, which includes both the time update step and measurement correction of $\boldsymbol{x}$ (Best et al., 2007).

$$\boldsymbol{F_k^*} = \boldsymbol{F}(\hat{\boldsymbol{x}}_\boldsymbol{k}) - \boldsymbol{S}\boldsymbol{R^{-1}}\boldsymbol{H}(\hat{\boldsymbol{x}}_\boldsymbol{k}) \tag{8}$$

$$\boldsymbol{K_k} = \boldsymbol{P_k}\boldsymbol{H^T}(\hat{\boldsymbol{x}}_\boldsymbol{k})[\boldsymbol{H}(\hat{\boldsymbol{x}}_\boldsymbol{k})\boldsymbol{P_k}\boldsymbol{H^T}(\hat{\boldsymbol{x}}_\boldsymbol{k}) + \boldsymbol{R}]^{-\mathbf{1}} \tag{9}$$

$$\boldsymbol{P_k^*} = [\boldsymbol{I} - \boldsymbol{K_k}\boldsymbol{H}(\hat{\boldsymbol{x}}_\boldsymbol{k})]\boldsymbol{P_k} \tag{10}$$

$$\boldsymbol{P_{k+1}} = \boldsymbol{P_k^*} + \Delta\boldsymbol{t}[\boldsymbol{Q} - \boldsymbol{S}\boldsymbol{R^{-1}}\boldsymbol{S^T} + \boldsymbol{F^*}(\hat{\boldsymbol{x}}_\boldsymbol{k})\boldsymbol{P_k^*} + \boldsymbol{P_k^*}\boldsymbol{F^{*T}}(\hat{\boldsymbol{x}}_\boldsymbol{k})] \tag{11}$$

$$\hat{\boldsymbol{x}}_{\boldsymbol{k+1}} = \hat{\boldsymbol{x}}_\boldsymbol{k} + \boldsymbol{K_k}\big(\boldsymbol{y_k} - \boldsymbol{h}(\hat{\boldsymbol{x}}_\boldsymbol{k})\big) + \Delta\boldsymbol{t}[\boldsymbol{f}(\hat{\boldsymbol{x}}_\boldsymbol{k}) + \boldsymbol{S}\boldsymbol{R^{-1}}\big(\boldsymbol{y_k} - \boldsymbol{h}(\hat{\boldsymbol{x}}_\boldsymbol{k})\big)] \tag{12}$$

where $\hat{\boldsymbol{x}}_\boldsymbol{k}$is the system estimate, $\boldsymbol{F}(\hat{\boldsymbol{x}}_\boldsymbol{k})$and $\boldsymbol{H}(\hat{\boldsymbol{x}}_\boldsymbol{k})$are the Jacobian of $\boldsymbol{f}(\boldsymbol{x_k}, \boldsymbol{u_k}, \boldsymbol{\Theta}_\mathbf{k})$ and $\boldsymbol{h_k}(\boldsymbol{x_k})$ respectively, $\boldsymbol{K_k}$ is the Kalman gain, and $\Delta\boldsymbol{t}$ is the sample time between instants $\boldsymbol{t_k}$ and $\boldsymbol{t_{k+1}}$. The matrices $\boldsymbol{P}$, $\boldsymbol{Q}$, $\boldsymbol{R}$ and $\boldsymbol{S}$ are error covariance matrices associated with the estimate, the model's prediction, sensor measurement, and cross measurement-process respectively (Best et al., 2000).

One can then identify parameters of the system by augmenting the state vector estimated by the EKF as $\bar{\boldsymbol{z}} = [\boldsymbol{x}, \boldsymbol{\Theta}]^{\boldsymbol{T}}$. The dynamics of this augmented vector is described by

$$\dot{\bar{\boldsymbol{z}}} = \begin{bmatrix} \dot{\boldsymbol{x_k}} \\ \dot{\boldsymbol{\Theta}}_\mathbf{k} \end{bmatrix} = \begin{bmatrix} \boldsymbol{f}(\boldsymbol{x_k}, \boldsymbol{u_k}, \boldsymbol{\Theta}_\mathbf{k}) \\ \mathbf{0} \end{bmatrix} + \begin{bmatrix} \boldsymbol{w_x} \\ \boldsymbol{w_\Theta} \end{bmatrix} \tag{13}$$

Where $\boldsymbol{w_\Theta}$ is the uncertainty associated with the parameters $\boldsymbol{\Theta}$.

Equation (13) indicates that the estimated parameters are assumed to be constants in the real system, if $\boldsymbol{w_\Theta}$ is defined as zero. As such, in this implementation of the EKF, parameters will converge to their correct values as a result of the measurement update step, rather than as result of time propagation step. As a result, the parameter convergence dynamics are slower than the system's state propagation dynamics (Best et al., 2007).

3.2 Application on the MuSat Platform

In this work, the EKF will be used for estimating the inertia matrix $\boldsymbol{I_{system}}$ elements and the position of the center of mass $\boldsymbol{r_{CM}} = [r_x, r_y, r_z]^{\boldsymbol{T}}$. The function $\boldsymbol{f}(\boldsymbol{x_k}, \boldsymbol{u_k}, \boldsymbol{\Theta}_\mathbf{k})$ can be derived from Eq. (3), Eq. (4) and Eq. (5). Therefore, the state vector estimated by the filter must be defined as $\boldsymbol{x} = [\phi\ \theta\ \psi\ \omega_x\omega_y\omega_z r_x r_y r_z I_{xx} I_{yy} I_{zz,} I_{yz} I_{xz} I_{xy}]^{\boldsymbol{T}}$, where I_{xx} , $I_{yy}, I_{zz,}, I_{yz}$, I_{xz}, I_{xy} are components of the inertia matrix. To initialize the filter, it is necessary to provide an initial value for these parameters, from which they will converge towards the identified values. All system variables are initially assumed to be at the origin, while the CAD values of the moment of inertia matrix are used as the initial guess for the EKF. The initial guess for the position of the center of mass is at the center of rotation of the sphere.

It is suggested in (Oliveira et al., 2013) and in (Sharifi and Zabihian, 2018) that due to the nonlinear nature of the satellite dynamics, all modes must be excited for obtaining an accurate measurement of the mass properties. Therefore, for exciting the system, the attitude controller (shown in the structure presented in Fig. 2) was modified so it commands the reaction wheels to generate an excitation input torque for each axis. The resulting attitude response data is then used on the filter, which will then estimate the values of the inertia matrix and the CM position.

4. RESULTS

The controller was then configured to generate a sinusoidal input torque for each one of the wheels. All wheels were continuously accelerated and decelerated from 1950 to 2050 RPM. The input sinusoid has a period of 120 seconds, generating up to 0.34408 mNm of torque on each axis. The phase delay between each sinusoid is of 120 degrees. Data was acquired at a rate of 0.2 seconds. This experiment lasted 300 seconds, acquiring 1501 samples.

Figure 3 shows the torque output and the velocity of each reaction wheel. Figure 4 shows the response measured by the sphere's IMU, in terms of attitude and angular velocity.

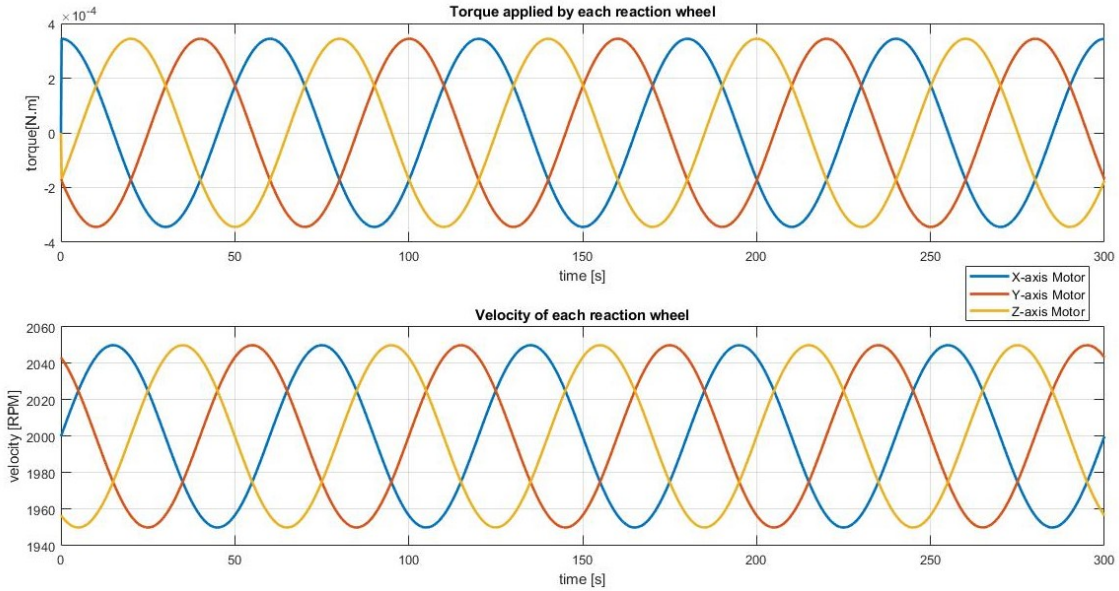

Figure 3. Reaction wheels' output torque and spinning velocity.

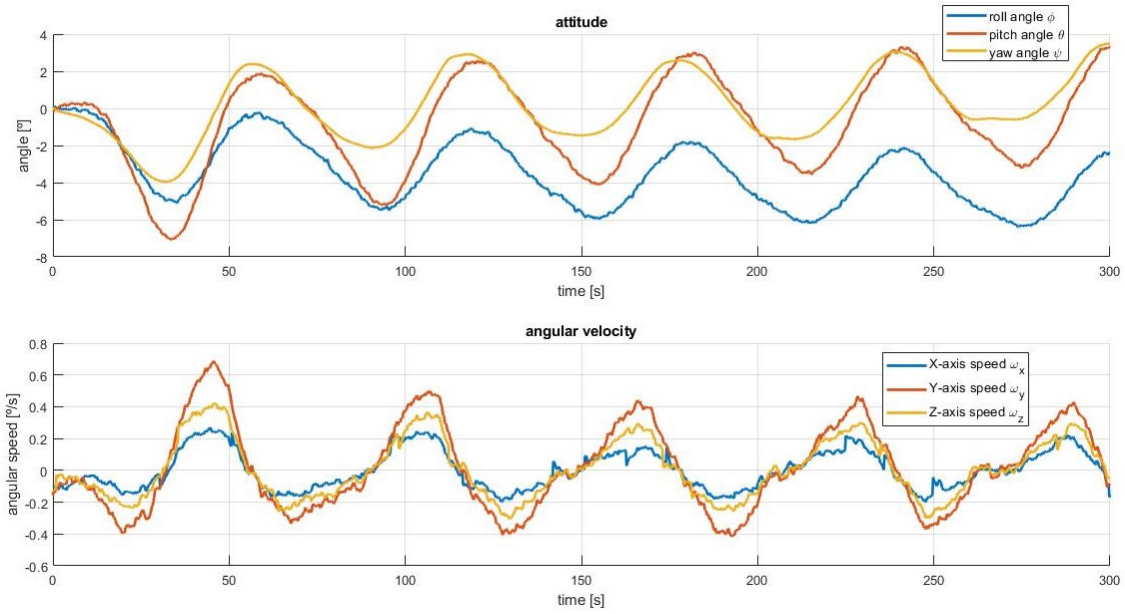

Figure 4. System response measured by the IMU.

By feeding the EKF with the data obtained from the experiment, the EFK provided a stable estimation of the current position of the center of mass and the current mass properties of the sphere. The parameters used for initializing the EFK can be seen on Tab. 1.

Table 1. Data used for initializing the EKF.

EKF parameter	Value
Initial attitude vector $[\phi\ \theta\ \psi]^T$(rad)	$[0\ 0\ 0]^T$
Initial angular velocity vector $\boldsymbol{\omega}$ (rad/s)	$[0\ 0\ 0]^T$
Initial center of mass position $\boldsymbol{r_{CM}}$ (m)	$[0\ 0\ 0]^T$
Initial moments of inertia $[I_{xx}I_{yy}I_{zz}]^T$(kg.m^2)	$[0.1358\ 0.1359\ 0.1227]^T$
Initial products of inertia $[I_{yz}I_{xz}I_{xy}]^T$(kg.m^2)	$[2.2952 \times 10^{-4} \quad -1.7439 \times 10^{-4} \quad -2.2908 \times 10^{-5}\ ]^T$
diag(Q)	$10^{-9}[0,0,0,1,1,1,0,0,0,0,0,0,0,0,0]^T$
diag(R)	$10^{-5}[0.1\ 0.1\ 0.1\ 1\ 1\ 1]^T$
Initial covariance *diag (P)*	$[10^{-1}, 10^{-1}, 10^{-1}, 10^{-1}, 10^{-1}, 10^{-1}, 10^{-7}, 10^{-7}, 10^{-7}, 10^{-5}, 10^{-5}, 10^{-5}, 10^{-4}, 10^{-4}, 10^{-4}]^T$

The parameters $\boldsymbol{P}$, $\boldsymbol{Q}$ and $\boldsymbol{R}$ of the EKF were not known a priori. Simulation work performed in (Oliveira et al., 2013) indicated that the choice of these parameters have a large impact on parameter estimation performance. Therefore, a strategy for choosing these parameters was devised.

First, $\boldsymbol{Q}$ and $\boldsymbol{P}$ were set to extremely small values in comparison to $\boldsymbol{R}$. This causes the EKF to practically ignore the measurement update step and prevents the estimated parameters from varying over time, as all measurements are assumed to have very high uncertainty in comparison with the predictions obtained from the model. This procedure allows one to verify the soundness of the underlying prediction model contained in the EKF.

After verifying that the underlying dynamical model of the EKF is functional, $\boldsymbol{Q}$ and $\boldsymbol{P}$ and were then manually and gradually increased up to the values in listed in Tab.1, for which the EKF yielded stable parameter estimations.

The results obtained from the estimation process can be seen on Fig. 5, with the final estimated parameters listed on Tab. 2.

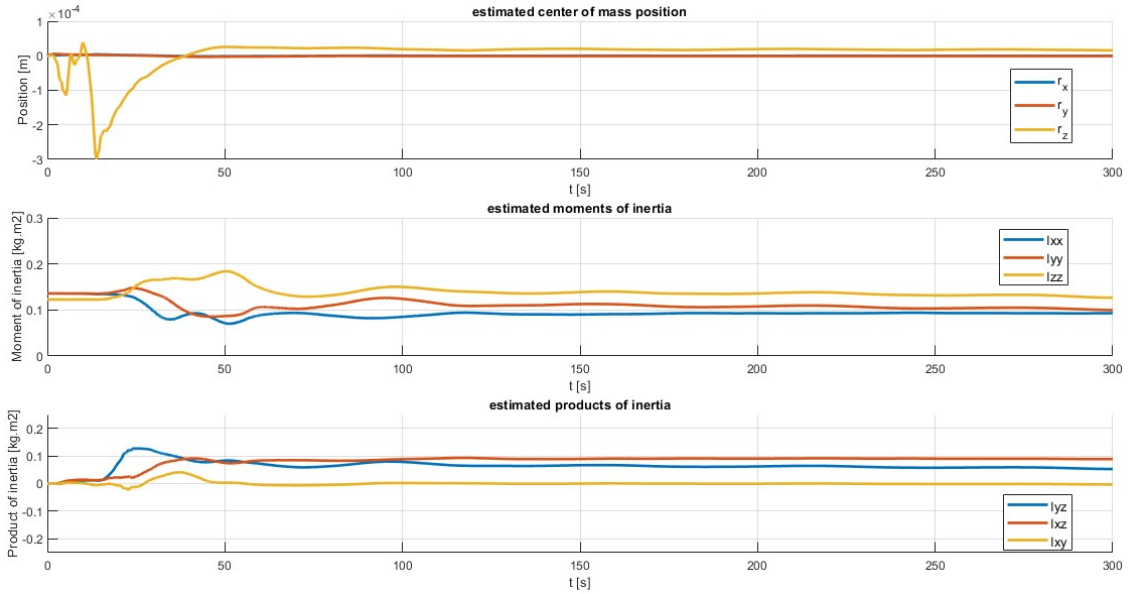

Figure 5. Properties estimated by the EKF.

Table 2. Mass characteristics estimated by the EKF.

Estimated Parameter	Value
I $\boldsymbol{r_{CM}}$ (m)	$[-8.356 \times 10^{-8} - 9.742 \times 10^{-7}\ 1.576 \times 10^{-5}]^T$
Moments of inertia $[I_{xx}I_{yy}I_{zz}]^T$(kg.m^2)	$[0.09309 \quad 0.09959 \quad 0.1265]^T$

Products of inertia $[I_{yz} I_{xz} I_{xy}]^T$ (kg.m^2)	$[0.05248 \quad 0.0886 \quad -0.003276]^T$

In order to validate the estimated parameters, the dynamical model presented in Eq. (3) was simulated using the same inputs used on the experiment and incorporating the parameters estimated by the EKF.

Figure 6 and Fig. 7 shows the simulation results, for attitude and angular velocity response over time. It can be seen on both plots that the model using the estimated parameters (marked in solid orange) provided a reasonably good fit for the experimental results (marked in dotted blue), although slightly out of phase.

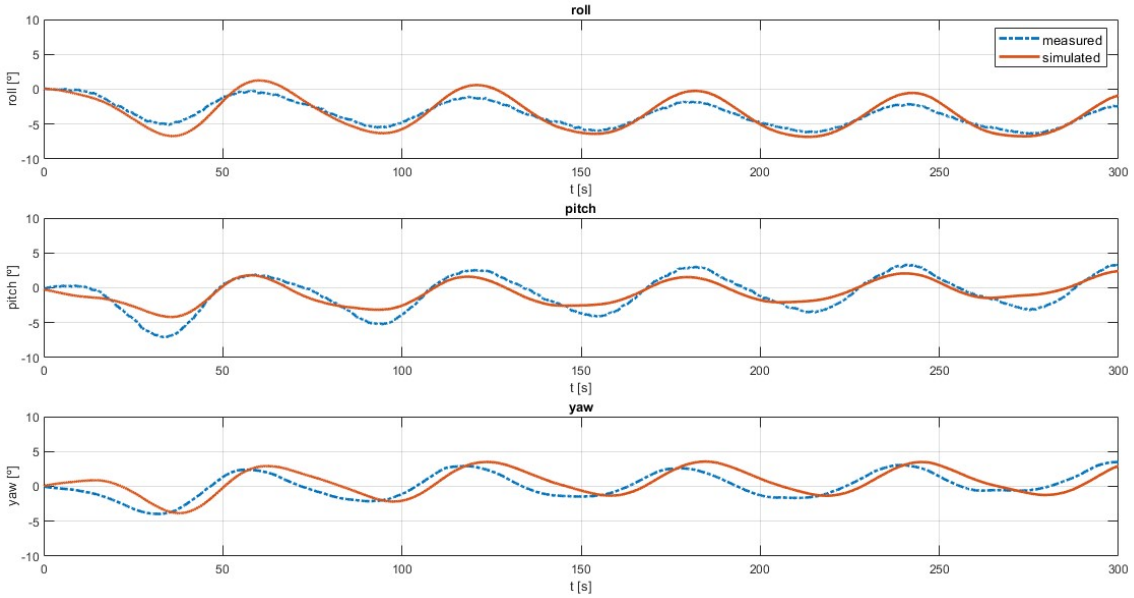

Figure 6. Attitude response of the simulated model using the estimated parameters.

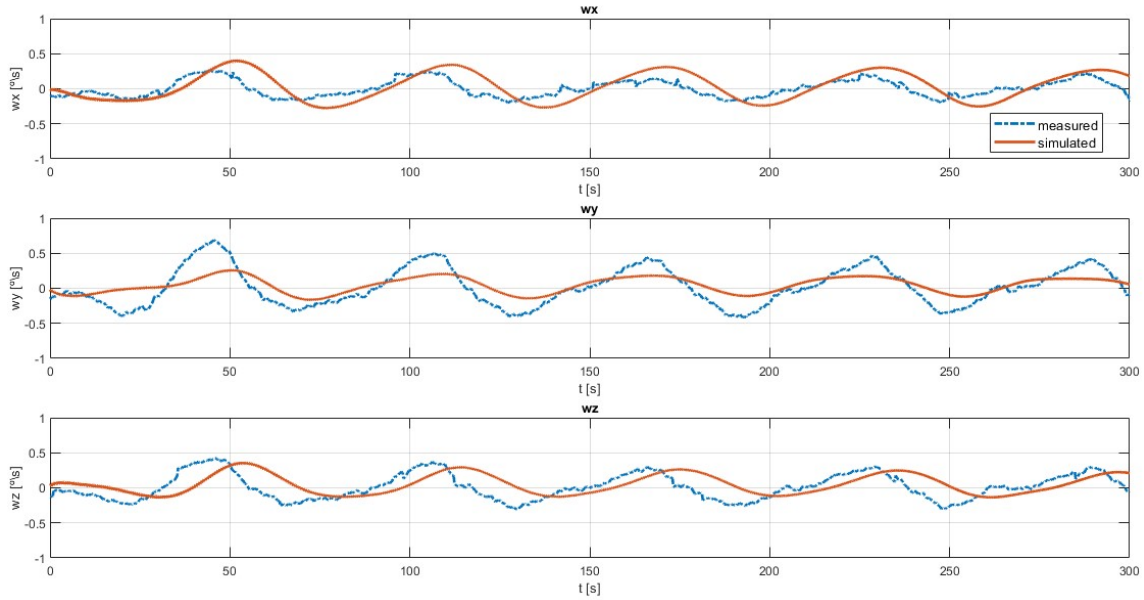

Figure 7. Angular velocity response of the simulated model using the estimated parameters.

5. CONCLUSION

This work presented the experimental application of the extended Kalman filter for identifying the mass properties of the MuSat satellite attitude dynamics simulator. The results obtained indicate that the attitude dynamics equations are sufficient to estimate the mass properties of the system. However, the parameters of the filter, such as the initial covariance matrix $\boldsymbol{P}$, model covariance matrix $\boldsymbol{Q}$ and measurement error covariance matrix $\boldsymbol{R}$ had to be defined empirically, which yielded a slightly delayed dynamics in our simulations in comparison with the experimental results.

We believe that a better choice of the filter parameters may lead to a more precise estimation of parameters, especially regarding the products of inertia of the system.

For future works, it is suggested devising an automated and/or optimized procedure for defining the extended Kalman filter initialization parameters, so that the parameters estimated by the EKF converge to their correct values at a minimum desired rate.

6. ACKNOWLEDGEMENTS

The authors are grateful for the funding of CAPES and CNPq, as well as all those involved in the preparation of this article.

7. REFERENCES

Best, M.C., Newton, A.P., and Tuplin, S. 2007. “The identifying extended Kalman Filter: parametric system identification of a vehicle handling model”. In *Proceedings of the Institution of Mechanical Engineers, Part K: Journal of Multibody Dynamics.* Pp 87-98.

Best, M.C., Gordon, T.J and Dixon, P.J., 2000. “An Extended Kalman Filter for Real-time State Estimation of Vehicle Handling Dynamics”. *Vehicle system Dynamics,* Vol 34, No. 1, pp 57-75.

Costa, R.F., and Saotome, O., 2016. “Satellite Attitude Control System Validation in an Air Beared Sphere”. In *Proceedings of 2nd Brazilian Technology Symposium - BTSYM’16.* Campinas, Brazil.

Costa, R.F., and Saotome, O., 2018. “Efficacy Comparison of Satellite Attitude Control Algorithms Using a Spherical Air Bearing”. In *Proceedings of the 4th Brazilian Technology Symposium - BTSYM’18*. Campinas, Brazil.

Figueiredo, H. and Saotome, O., 2013. “Design of a Set of Reaction Wheels for Satellite Attitude Control Simulation”. In *Proceedings of the 22nd International Congress of Mechanical Engineering – COBEM 2013*. Ribeirão Preto, Brazil.

Oliveira, A.M., Kuga, H.K., Carrara, V., 2013. ”Estimating the Mass Characteristics of a Dumbbell Air Bearing Satellite Simulator”.In *Proceedings of the 22nd International Congress of Mechanical Engineering – COBEM 2013*. Ribeirão Preto, Brazil.

Sharifi, G. and Zabihan. E., 2018. ”An Effective Approach To Identify The Mass Properties Of A Satellite Attitude Dynamics Simulator”. *Australian Journal of Mechanical Engineering*. Pp 2204-2253.

Sidi, M. J., 1997. *Spacecraft Dynamics and Control: A Practical Engineering Approach.*Cambridge University Press, Cambridge.

Silva, M. de A.C., Figueiredo, H.V., Boglietti, B.G.N., Saotome, O., Villani, E., Kienitz, K.H., 2014. “A Framework for Development of Satellite Attitude Control Algorithms”. *Journal of Control, Automation & Electrical Systems.* Vol. 25, No. 6, pp 657-667.

8. RESPONSIBILITY NOTICE

The authors are the only responsible for the printed material included in this paper.